Flow dynamics and forces associated with a cylinder rolling along a wall

Bronwyn Stewart, Kerry Hourigan, and Mark Thompson
Fluids Laboratory for Aeronautical and Industrial Research (FLAIR), Department of Mechanical Engineering, Monash University, Clayton, 3800, Australia

Thomas Leweke
Institut de Recherche sur les Phénomènes Hors Equilibre, CNRS/Universités Aix-Marseille, 49 Rue Frédéric Joliot-Curie, BP 146, F-13384 Marseille Cedex, France

(Received 8 July 2006; accepted 28 September 2006; published online 1 November 2006)

The wake flow structures and the drag force for a cylinder rolling along a wall without slipping were calculated for the Reynolds number range $20<\mathrm{Re}<200$, covering the two-dimensional shedding regime. Time-dependent numerical computations show the wake undergoes a steady to periodic shedding transition between $85<\mathrm{Re}<90$. The Strouhal number varies only weakly at higher Reynolds number, and is a factor of 3–4 lower than for an isolated rotating or nonrotating body. Also, within this shedding regime, the wake is characterized by counter-rotating vortex pairs, which propagate away from the wall via mutual induction. These pairs are formed as compact vortex structures from the top separating shear layer induce secondary vorticity at the wall, which is pulled up from the boundary to form the semidiscrete flow structures. Over both the steady and unsteady regimes, the (time-mean) recirculation length and drag are quantified. © *2006 American Institute of Physics*. [DOI: 10.1063/1.2375062]

The flow structures which form around a bluff body have been shown to vary dramatically with both the introduction of rotation,[1–4] and the influence of nearby walls.[5–7] However, few studies have considered these two effects acting in tandem, such as occurs when a body is rolling along a surface. The work of Zeng *et al.*[8] examined the translating motion of a sphere along a plane wall when it was permitted to rotate freely. Relatively small rotation rates could be induced by the flowing fluid, which had a minimal effect on the lift and drag forces experienced by the sphere. For the more fundamental, two-dimensional problem of the rolling cylinder, Bhattacharyya *et al.*[9] undertook a study using a numerical code which enforced steady flow. Unfortunately, this allowed no information to be obtained relating to the unsteady flow regimes that may exist. Furthermore, at low Reynolds numbers, Re, the regions of steady, recirculating flow resembled highly viscous creeping flow and differed significantly in both size and shape to those observed for a sliding bluff body near a wall at similar Re.[10]

In order to clarify the nature of this unsteady transition, the current research utilized two-dimensional time-dependent numerical simulations of a cylinder rolling along a plane wall to investigate the flow transitions occurring for $20 \leqslant \mathrm{Re} \leqslant 200$, with Re based on the cylinder diameter, D, and the translational velocity, U. This range covers the regime of attached, recirculating flow at the back of the cylinder into the vortex shedding regime. For this study, the nondimensional rotation rate was defined as $\alpha=\omega D/2U$, where ω is the angular velocity of the cylinder.

For a stationary isolated cylinder in uniform flow, the stagnation point attaches to the front of the body. However, for $\alpha=0.5$ and above, the stagnation point moves off the surface of the cylinder,[11] and at higher rotation rates the cylinder entrains a layer of rotating fluid, thereby preventing attachment of the stagnation point to the body.[2,12] At a critical value of the rotation rate, the shedding is suppressed altogether. This critical rotation rate is dependent on Re but has been found to plateau at approximately $\alpha=2$.[4,12,13] As a nonrotating cylinder in a uniform flow moves into the proximity of the wall, the wake becomes asymmetric as the shear layer nearest the wall is suppressed. This results in a weakening of the shed vortices and can eliminate vortex shedding entirely.[5,6,10] It is expected that the reduction in shed vorticity observed in previous studies, due to both body rotation and wall proximity, will in turn diminish three-dimensional effects and provide a good approximation to two-dimensional flow up to the maximum Re studied.

Past experiments have shown that when the relative density of the body is taken into consideration, it is possible for a reversed rotation to exist (when the relative velocities of the body and the wall are opposite in direction at their nearest point). This is particularly relevant for falling spheres and occurs when the body is suspended above the surface due to the lift force exerted by the flow.[14,15] However, the current study focuses on the important limiting case of pure rolling when no-slip is present between the body and the wall. For this reason, α was fixed at unity, with the tangential velocity of the cylinder surface equal to U.

A schematic of the flow and geometry presently under consideration is shown in Fig. 1, with the body rolling with $\alpha=1$. All results have been obtained using a two-dimensional spectral element code with simulations carried out in the frame of reference attached to the center of the cylinder. The mesh used consisted of approximately 550 macroelements with a total distance of $100D$ to the upstream and downstream boundaries and $150D$ to the cross-stream boundary, with all measurements taken from the cylinder center, providing a blockage ratio of less than 1%. Seventh order

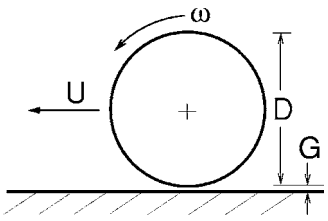

FIG. 1. Schematic showing the rotation and translation of the cylinder in the laboratory reference frame.

($N=8$) Lagrangian polynomials were fitted to each macro element of the mesh to solve for the relevant variables at the $N\times N$ points. A more detailed explanation of the code can be found in Thompson *et al.*[16] These mesh parameters were considered to provide adequately converged solutions, with further increases in N or domain size giving a variation in St and the mean lift and drag within 0.1% for Re=200.

To prevent divergence of the numerical code, it was not possible to position the cylinder in contact with the wall as the elements became degenerate at the point of contact. To overcome this, the cylinder boundary was offset by a small distance, G. The pressure gradient through this gap was found to increase as $G/D\rightarrow 0$, where G/D will henceforth be referred to as the gap ratio. This was consistent with experimentally observed lubrication effects which lead to cavitation.[17] Pressures developed on the body away from the gap displayed very little change with small variations in $G/D<0.01$. This was reflected in the flow structures developing around the body and the streamlines of the flow, which also showed no discernible change. In order to maintain stability and reduce computing times, a gap ratio of 0.005 was chosen to approximate the case of the body in contact with the wall. The streamlines in this region showed the formation of a narrow jet of fluid either side of the gap and closely resembled the analytical solution of Bhattacharyya *et al.*[9] for the body in contact with the wall. For unsteady flow at Re=200, St varied only weakly linearly with G/D. Extrapolation of the results to $G/D=0$ showed St to be within 2.5% of the calculated value at $G/D=0.005$.

Vorticity contours were plotted to show the downstream wake structures and results are shown in Fig. 2 for Re=50, 100, 150, and 200. The flow experiences a Hopf bifurcation at $\mathrm{Re}\approx 87$. This is somewhat higher than the transition values between $50<\mathrm{Re}<54$ found in previous studies for the isolated rotating and translating cylinder with $\alpha=1$.[11,13,18] This delay in the onset of unsteady flow is attributed to the stabilizing effect provided by the wall, as observed by Arnal *et al.*[10] for the square sliding body and Reichl *et al.*[19] for a cylinder near a free surface with Fr=0.

Prior to the transition to unsteady flow, the flow downstream of the body is characterized by fixed regions of recirculating fluid. The largest of these regions rotates in the clockwise direction and is formed by the flow passing over the top of the cylinder. This is indicated by the large region of negative vorticity in Fig. 2(a). A smaller region of anticlockwise recirculation is generated closer to the wall at higher Re by the flow being pulled in at the back of the cylinder. Vorticity generated in this region near the plane

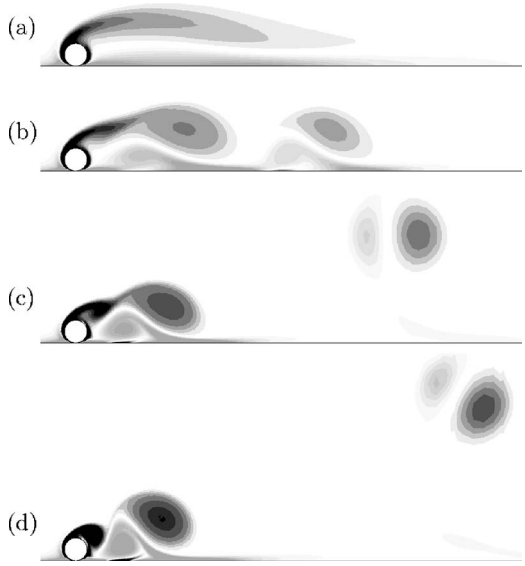

FIG. 2. Instantaneous vorticity contours at moment of maximum lift force for (a) Re=50, (b) Re=100, (c) Re=150, and (d) Re=200. Negative vorticity is shown in dark gray.

wall rolls up and pairs with the vorticity generated on the surface of the cylinder [shown in Figs. 2(b)–2(d)]. Reduced diffusion and cross-annihilation at higher Re preserves the strength of the individual vortices, resulting in the shed pair being propelled further from the wall as Re increased.

The time-averaged velocity fields were obtained for all Re. These were then used to measure the average length of the dominant recirculation region behind the body, L^*, as measured downstream from the cylinder center and normalized by D. The length of these regions provide an indication of the area behind the body in which the shear layers and vortical structures interact with the wall. This parameter has implications for fluid mixing and heat transfer as well as possible suspension or deposition of particles within the flow.

The recirculation regions were defined by closed streamlines and the resulting values of L^* are shown in Fig. 3. During steady flow, the recirculation length increases linearly from $L^*=2.9$ at Re=20, until the transition Re was reached. This linear trend provides a valuable comparison and is con-

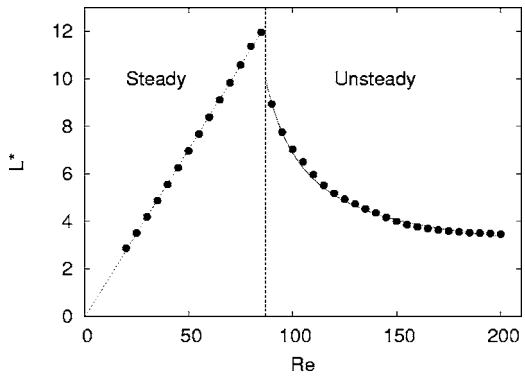

FIG. 3. Average values of the normalized length, L^*, for the upper recirculation region before and after the unsteady transition.

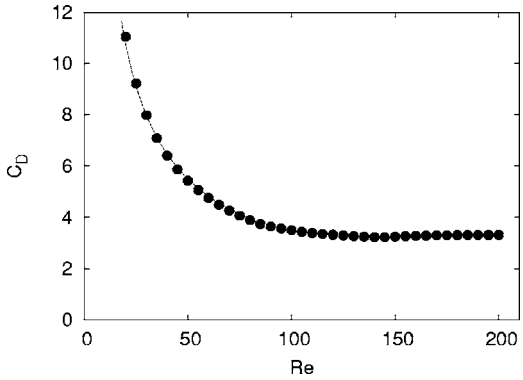

FIG. 4. Coefficient of drag for the rolling body with $G/D=0.005$. The functional fit shown for the steady data (−) was of the form $C_D=A\,\mathrm{Re}^B$, where $A=101.18$ and $B=-0.7457$. This fitted curve had an error of less than 2%.

sistent with other studies of recirculation regions behind bodies in laminar flow.[20,21] In the unsteady flow regime, the recirculation lengths obtained from the time-mean flow fields were observed to decrease as $L^*=148.59(\mathrm{Re}-67.88)^{-1}+2.26$. This fit is shown in Fig. 3 and was accurate to within 4%. As all simulations were started impulsively from rest, very long time-scale simulations were required to obtain steady-state solutions near the bifurcation point. This bifurcation is shown in Fig. 3 as the vertical line at Re=87.

The time-average drag coefficients were calculated for a gap ratio of $G/D=0.005$ and are shown in Fig. 4. In the steady flow regime, C_D decreases smoothly according to a power relationship of the form $C_D=A\,\mathrm{Re}^B$ as Re is increased. This fit is shown in Fig. 4, along with the corresponding values of A and B for $G/D=0.005$.

The periodic shedding of the flow at Re>87 is illustrated in Fig. 5 for Re=200. These vorticity contours are presented over one period of shedding and show the movement of the shed vortices as the body rolls towards the left. At this Reynolds number, the shear layer vorticity shedding from the cylinder rolls up into a strong, compact vortical structure. In turn, this induces opposite-signed vorticity at the boundary which is lifted from the wall to form a counter-rotating vortex pair, similar to that observed by Arnal *et al.*[10] The unequal strength of the two vortices results in a net clockwise rotation around the strongest vortex as they propel away from the wall. The instantaneous vorticity and streamlines generated at the cylinder surface for Re=200 are shown more clearly in Fig. 6. Figure 6(a) shows the large magnitude vorticity generated over the lower half of the cylinder and the adjacent wall, while Fig. 6(b) shows the instantaneous recirculation region formed over the top of the cylinder.

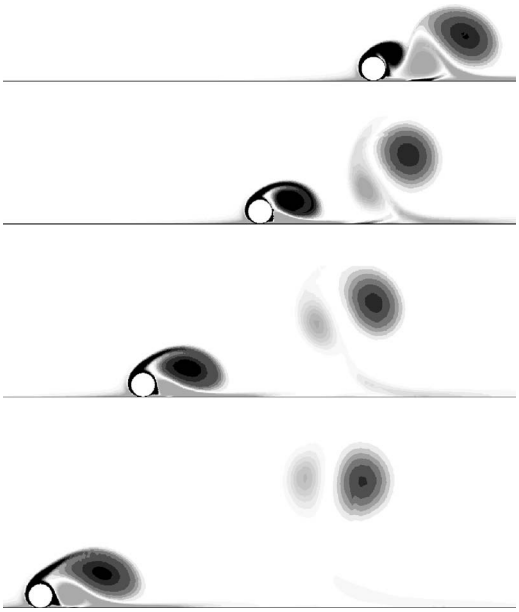

FIG. 5. Position of shed vortices for Re=200 over one shedding cycle, in the *fixed* reference frame.

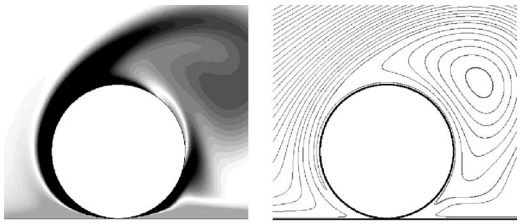

(a) Vorticity (b) Streamlines

FIG. 6. Instantaneous flow structures at Re=200.

Two critical points exist in the flow, just upstream and downstream of the point of nearest proximity of the body to the wall. These are stagnation points, the positions of which are reflected in earlier work by Bearman and Zdravkovich[5] who found that the stagnation point moved towards the gap region as G/D was reduced. This was directly attributed to the pressure gradient formed by flow between the body and the wall.

In the unsteady flow regime, St ranges from 0.065 at Re=95 and decreases gradually up to the maximum Re considered, Re=200. This is shown in Fig. 7, along with the Strouhal number relationships for the translating and rotating cylinder in a free-stream. From this it can be seen that the experimental results of Williamson[22] for the nonrotating cylinder coincide closely with the results of Kang *et al.*[11] and

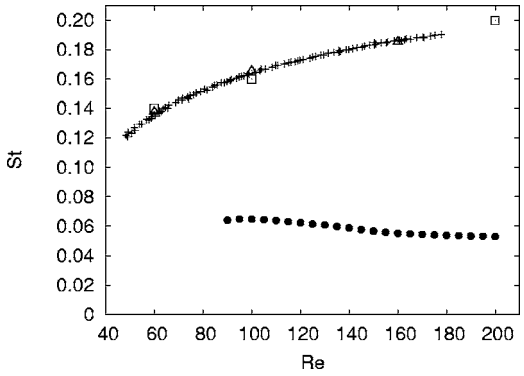

FIG. 7. Comparison of shedding frequency for: ●, the present study with the rolling body on the wall; +, results of Williamson (Ref. 22) for the isolated body with no rotation; △, from Kang *et al.* (Ref. 11) and □, from Badr *et al.* (Ref. 23) with the latter two calculated for the rotating body in a free-stream with $\alpha=1$.

Badr *et al.*[23] for the rotating cylinder with $\alpha=1$ in a free-stream. This is in contrast to the current results which have significantly lower values of St. This wall effect is consistent with the findings of Arnal *et al.*[10] who observed a reduction in shedding frequency when the wall was present.

In the current study it was observed that the transition from a steady to time-varying flow occurs for $85<\mathrm{Re}<90$. Also, the period of vortex shedding is significantly reduced below that of the rotating body in the free-stream due to the effect of the wall. When Re was increased in the steady regime the length of the dominant recirculation region behind the body increased linearly. Further increase in Re brought about a transition to unsteady flow and a decrease in the mean recirculation length.

Further studies are being carried out to indicate to what extent (if any) three-dimensional effects are present in the flow. Also, to discover if it is possible, by independently varying the rotation rate of the body relative to its translation, to control the lift and drag forces exerted by the fluid on the cylinder.

This research was made possible through the support of ARC Discovery Grant No. DP0555897 and an Australian Postgraduate Award.

[1] H. M. Badr and S. C. R. Dennis, "Time-dependent viscous flow past an impulsively started rotating and translating circular cylinder," J. Fluid Mech. **158**, 447 (1985).
[2] M. Coutanceau and C. Ménard, "Influence of rotation on the near-wake development behind an impulsively started circular cylinder," J. Fluid Mech. **158**, 399 (1985).
[3] D. B. Ingham and T. Tang, "A numerical investigation into the steady flow past a rotating circular cylinder at low and intermediate Reynolds numbers," J. Comput. Phys. **87**, 91 (1990).
[4] S. Mittal and B. Kumar, "Flow past a rotating cylinder," J. Fluid Mech. **476**, 303 (2003).
[5] P. W. Bearman and M. M. Zdravkovich, "Flow around a circular cylinder near a plane boundary," J. Fluid Mech. **89**, 33 (1978).
[6] S. J. Price, D. Sumner, J. G. Smith, K. Leong, and M. P. Païdoussis, "Flow visualization around a circular cylinder near to a plane wall," J. Fluids Struct. **16**, 175 (2002).
[7] A. Dipankar and T. K. Sengupta, "Flow past a circular cylinder in the vicinity of a plane wall," J. Fluids Struct. **20**, 403 (2005).
[8] L. Zeng, S. Balachandar, and P. Fischer, "Wall-induced forces on a rigid sphere at finite Reynolds number," J. Fluid Mech. **536**, 1 (2005).
[9] S. Bhattacharyya, S. Mahapatra, and F. T. Smith, "Fluid flow due to a cylinder rolling along ground," J. Fluids Struct. **19**, 511 (2004).
[10] M. P. Arnal, D. J. Goering, and J. A. C. Humphrey, "Vortex shedding from a bluff body adjacent to a plane sliding wall," ASME J. Fluids Eng. **113**, 384 (1991).
[11] S. Kang, H. Choi, and S. Lee, "Laminar flow past a rotating circular cylinder," Phys. Fluids **11**, 3312 (1999).
[12] F. Díaz, J. Gavaldà, J. G. Kawakk, J. F. Keffer, and F. Giralt, "Vortex shedding from a spinning cylinder," Phys. Fluids **26**, 3454 (1983).
[13] J. F. Jaminet and C. W. Van Atta, "Experiments on vortex shedding from rotating circular cylinders," AIAA J. **7**, 1817 (1969).
[14] J. A. C. Humphrey and H. Murata, "On the motion of solid spheres falling through viscous fluids in vertical and inclined tubes," ASME J. Fluids Eng. **114**, 2 (1992).
[15] Y. J. Liu, J. Nelson, J. Feng, and D. D. Joseph, "Anomalous rolling of spheres down an inclined plane," J. Non-Newtonian Fluid Mech. **50**, 305 (1993).
[16] M. Thompson, K. Hourigan, and J. Sheridan, "Three-dimensional instabilities in the wake of a circular cylinder," Exp. Therm. Fluid Sci. **12**, 190 (1996).
[17] J. R. T. Seddon and T. Mullin, "Reverse rotation of a cylinder near a wall," Phys. Fluids **18**, 041703 (2006).
[18] G.-H. Hu, D.-J. Sun, X.-Y. Yin, and B.-G. Tong, "Hopf bifurcation in wakes behind a rotating and translating circular cylinder," Phys. Fluids **8**, 1972 (1996).
[19] P. Reichl, K. Hourigan, and M. C. Thompson, "Flow past a cylinder close to a free surface," J. Fluid Mech. **533**, 269 (2005).
[20] S. C. R. Dennis and G.-Z. Chang, "Numerical solutions for steady flow past a circular cylinder at Reynolds numbers up to 100," J. Fluid Mech. **42**, 471 (1970).
[21] P. T. Williams and A. J. Baker, "Numerical simulations of laminar flow over a 3D backward-facing step," Int. J. Numer. Methods Fluids **24**, 1159 (1997).
[22] C. H. K. Williamson, "Oblique and parallel modes of vortex shedding in the wake of a circular cylinder at low Reynolds numbers," J. Fluid Mech. **206**, 579 (1989).
[23] H. M. Badr, S. C. R. Dennis, and P. J. S. Young, "Steady and unsteady flow past a rotating circular cylinder at low Reynolds numbers," Comput. Fluids **17**, 579 (1989).